

## Reexamination of $\beta$ -Alumina Doped with Chromium Using Photoacoustic Spectroscopy

JOHN H. KENNEDY AND ANN M. SCHULER

*Chemistry Department, University of California,  
Santa Barbara, California 93106*

AND GEORGE E. CABANISS

*Chemistry Department, University of North Carolina,  
Chapel Hill, North Carolina 27514*

Received November 11, 1982; in revised form March 21, 1983

A previous publication presented evidence that supported the hypothesis that chromium-doped  $\beta$ -alumina was oxidized to Cr(IV) during air-sintering. This evidence included chemical reactions observed, magnetic susceptibility, and conductivity, but, in particular, the strongest supporting evidence came from absorption spectroscopy. However, the technique used, powder dispersed in a KBr pellet, was not conducive to high quality spectra. For this reason, a much more powerful technique for solid samples, photoacoustic spectroscopy, has been applied to chromium-doped  $\beta$ -alumina. Additional absorption peaks have been observed that now clearly show that chromium remains as Cr(III) in  $\beta$ -alumina. The other previous evidence has been reexamined and it too can be interpreted as resulting from the presence of chromium(III).

### Introduction

A previous publication from our laboratory (1) presented evidence that supported the hypothesis that chromium-doped  $\beta$ -alumina was oxidized to Cr(IV) during air-sintering. Briefly, this evidence can be summarized as follows.

The first indication of an oxidation state change came from observed color changes taking place when the samples were treated with 90% N<sub>2</sub>/10% H<sub>2</sub> at 1200°C. The air-sintered materials were green while the treatment with H<sub>2</sub> converted the material to a pink color. The pink material exhibited spectral characteristics nearly identical to ruby, i.e., Cr(III) in Al<sub>2</sub>O<sub>3</sub>. X-ray diffrac-

tion of both the pink and green forms showed lines attributable to  $\beta$ -alumina. It should be noted at this point that the powder camera used in this early study had no filter for  $K_{\beta}$  radiation. Because of their close proximity,  $K_{\alpha}$  lines of  $\alpha$ -Al<sub>2</sub>O<sub>3</sub> could be interpreted as  $K_{\beta}$  lines of  $\beta$ -alumina. Color change in itself would not necessarily involve an oxidation state change so other measurement probes were utilized. Magnetic susceptibility measurements were taken on both the green and pink forms. Magnetic moments were low, which is common for metal oxides even when present in dilute solid solution, but the difference in magnetic moment between the green and pink forms was 1.57 B.M. This

was more than enough for a one-electron change. Because the spectral evidence was so strong (both absorption and emission spectroscopy) that the pink form was Cr(III), the magnetic susceptibility measurement supported the idea that the green form contained chromium in some higher oxidation state.

The third, and strongest, evidence supporting an assignment came from absorption spectrophotometry of both the green and pink forms. The powder was dispersed in a KBr pellet and two peaks were observed: 372 and 275 nm. On the other hand, the pink form exhibited peaks at 565 and 410 nm. Fits were attempted using Tanabe–Sugano diagrams. While the pink form fit a  $d^3$  configuration extremely well, the peaks observed for the green form could not be fit to a  $d^3$  assignment. However, they did fit a  $d^2$  assignment, which would be expected for Cr(IV).

Finally, the conductivity of the green form was somewhat lower than undoped  $\beta$ -alumina (2). This would be expected for a M(IV) dopant because fewer conductive sodium ions may be present for charge neutralization. Alternatively, additional interstitial oxide ions that could block  $\text{Na}^+$  conduction may be present to accomplish charge compensation.

With the advent of modern photoacoustic spectroscopy, a powerful tool for observing absorption peaks in polycrystalline solid materials has become available (3), and a reexamination of  $\beta$ -alumina doped with chromium was carried out.

## Experimental

**Sample preparation.** Pure Alcoa XB-2 superground  $\beta$ -alumina was doped by the addition of chromium nitrate [ $\text{Cr}(\text{NO}_3)_3 \cdot 9\text{H}_2\text{O}$ ], chromium oxide ( $\text{Cr}_2\text{O}_3$ ), or chromium oxalate [ $\text{Cr}_2(\text{C}_2\text{O}_4)_3 \cdot 4\text{H}_2\text{O}$ ], within the concentration range of 1 to 15 wt%. Powders having Cr concentrations of 1, 2, 4

wt% were doped using the nitrate. For dopant levels  $>4$  wt%  $\text{Cr}_2\text{O}_3$  or  $\text{Cr}_2(\text{C}_2\text{O}_4)_3 \cdot 4\text{H}_2\text{O}$  was used.

The pure  $\beta$ -alumina powder was thoroughly mixed with the Cr dopant using an  $\alpha$ -alumina mortar and pestle in an acetone slurry. One mole of anhydrous  $\text{Na}_2\text{CO}_3$  was added for every eight moles of  $M^{3+}$  added to the pure  $\beta$ -alumina. The acetone was allowed to evaporate and the powder was mixed well again to ensure a homogeneous distribution of metal dopant.

The mixed materials were placed in an  $\alpha$ -alumina crucible or boat and calcined in air at  $1000^\circ\text{C}$  for 24 hr. After calcination, the powder was again thoroughly mixed with an  $\alpha$ -alumina mortar and pestle.

The calcined doped  $\beta$ -alumina powder was then pressed to  $50 \times 10^3$  psi in a KBr steel punch and die. Each disk was then isostatically pressed to 25,000 psi. At this point average densities of isostatically pressed disks ranged from 2.2 to 2.35  $\text{g}/\text{cm}^3$ .

**Sintering.** The pressed disks were packed in a Coors porcelain high purity (99.8%  $\text{Al}_2\text{O}_3$ ) cylindrical crucible, separated from one another by 320 mesh coarsely ground  $\beta$ -alumina.

Samples were sintered in an Astro Industries Inc. furnace. Samples containing concentrations of  $\text{Cr} \leq 4$  wt% were sintered at  $1600^\circ\text{C}$  for 3 hr. Those having Cr concentrations  $\geq 4$  wt% were sintered between  $1750$  and  $1800^\circ\text{C}$  for 3.5 hr. The high sintering temperatures for the highly doped samples ( $\geq 6$  wt%) were needed to achieve densities close ( $\sim 98\%$ ) to theoretical.

**Electrode deposition.** Electrodes were deposited on the polished samples using a Technics Inc. Hummer sputtering apparatus using gold as a target. Electrode thickness was approximately 40 nm.

**Magnetic susceptibility.** Magnetic susceptibility measurements were made using a Cahn Electrobalance at  $298^\circ\text{K}$ . The susceptibility standard used was ferrous ammonium sulfate,  $\text{Fe}(\text{NH}_4)_2(\text{SO}_4)_2 \cdot 6\text{H}_2\text{O}$ .

Corrections were made for the diamagnetism of pure  $\beta$ -alumina.

*X-ray diffraction.* Both sintered samples and powders of doped  $\beta$ -alumina were checked for the presence or absence of the  $\beta$ -phase, changes in lattice parameters, and formation of second phases with a Philips X-ray diffractometer using a Debye-Scherrer camera and chromium radiation.

A Philips Electronic Instruments X-ray diffraction system with a Philips type 52572 scintillation counter employing copper ( $K\alpha$ ) radiation was also used to determine the presence or absence of the  $\beta$  phase in some samples.

*Reduction of Cr- $\beta$ -alumina.* Reduction of the resulting green powder was attempted using the following methods.

(i) The Cr-doped  $\beta$ -alumina powder was placed in a Coors  $\alpha$ - $\text{Al}_2\text{O}_3$  boat and heated to 1250°C in a Lindberg tube furnace for 24 hours under 10%  $\text{H}_2/90\%$   $\text{N}_2$  gas. The resulting powder was pink in color.

(ii) The doped powder was placed in the center of an  $\alpha$ - $\text{Al}_2\text{O}_3$  boat with coarse ground  $\beta$ -alumina on each side. The Cr- $\beta$ -alumina was separated from the coarse  $\beta$ -alumina by small stainless steel screens. The purpose of the coarse  $\beta$ -alumina was to provide an atmosphere of  $\text{Na}_2\text{O}$ , thus preventing soda loss from the doped material. The powders were heated to 1250°C for 36 hr under 10%  $\text{H}_2/90\%$   $\text{N}_2$  gas.

(iii) Green 2 wt% Cr-doped  $\beta$ -alumina was packed into the center of a small  $\alpha$ - $\text{Al}_2\text{O}_3$  tube with coarsely ground  $\beta$ -alumina enriched with  $\text{Na}_2\text{CO}_3$  added on both sides. Stainless steel screens separated the coarse  $\beta$ -alumina from the doped material. Plugs of  $\text{Al}_2\text{O}_3$  insulating felt were placed in each end of the tube. The tube assembly was placed in a Lindberg tube furnace and heated to 1150–1350°C for 24 to 60 hr under rapidly flowing 10%  $\text{H}_2/90\%$   $\text{N}_2$  gas. Results are given in Table I.

*Sodium analysis.* Sodium analysis was carried by the following two methods.

(i) Sodium content in sintered samples was determined using an ion exchange method. Pellets were immersed in molten  $\text{AgNO}_3$  overnight, rinsed in distilled water and dilute  $\text{HNO}_3$ , and then reimmersed in fresh molten  $\text{AgNO}_3$  for approximately 24 hr. The samples were rinsed again and then baked at 300°C overnight. Percent sodium in each sample was then found from the weight change that had occurred.

(ii) A flame emission technique was used with samples finely ground and dissolved in boiling 85%  $\text{H}_3\text{PO}_4$ . The dissolved powder was then diluted with distilled  $\text{H}_2\text{O}$  to a constant volume. Standard solutions were also prepared in the same manner.

Flame emission measurements were carried out with a Jarrell-Ash spectrometer using a hydrogen/air flame. The percent sodium was calculated from a standard calibration curve using pure  $\beta$ -alumina with known sodium content as a reference in the concentration range 10 to 750 mg/liter. All results shown in Table I for powder treated with  $\text{H}_2/\text{N}_2$  were carried out by flame emission. Previous studies (2) have shown that the two methods give equivalent results.

*Photoacoustic spectroscopy.* All photoacoustic spectra were acquired using a Princeton Applied Research Model 6001 photoacoustic spectrometer system which uses a 1-kW electronically pulsed xenon arc lamp in a F/4.2 reflector as its excitation source. System optics provide 8-nm resolution in the 200- to 800-nm spectral range when equipped with 2.0-mm exit and entrance slits. Detection of the photoacoustic signal is achieved by amplification of the microphone transducer. Real time source compensation is obtained by ratioing each analytical channel output to that of the pyroelectric detection system in parallel with the analytical channel.

The PAR 6001 system software has three storage channels available. A reference channel ( $R$ ) is used to store a spectrum of a black-body reference material (norite A,

TABLE I  
TEMPERATURE/TIME SCHEDULE FOR TREATMENT OF 2 W/O Cr  $\beta$ -ALUMINA POWDER WITH H<sub>2</sub>/N<sub>2</sub> GAS

Sample #	Total heating time (hr)	Temp. (max) (°C)	Color	Na (wt%)	% $\beta$ -alumina	Comments
#104R	36	1250	Pink	1.87	~0	2 wt% Cr- $\beta$ -powder placed in $\alpha$ -Al <sub>2</sub> O <sub>3</sub> boat
#101R	48	1200	Pink	1.05	~0	Same condition as above
#107-Cr-R	36	1250	Pink	1.52	27	6 wt% Cr-powder placed in $\alpha$ -Al <sub>2</sub> O <sub>3</sub> boat
#113-Cr-R	35	1280	Pink	2.2	45	Green 2 wt% Cr- $\beta$ -alumina packed in boat between coarse $\beta$ -alumina
#113-Cr-RIII	17	1250	Green	3.8	100	Green Cr- $\beta$ -alumina packed in tube between coarse $\beta$ -alumina
#113-Cr-RIII	18.5	1260	Green	3.8	100	Same sample as above heated an additional 18.5 hr, under same conditions
#113-Cr-RIII	24	1300	Green	3.6	100	Same sample as above heated 60 hr total
#113-Cr-RIV	18.5	1260	Green	3.8	100	2 wt% Cr- $\beta$ -powder (green) wrapped in Pt foil, placed in ceramic boat and covered with coarse $\beta$ -alumina
#113-Cr-RIV	24	1300	Green	3.5	100	Same condition as above

Fisher Scientific C-176). Signal-averaged spectra of undoped and doped  $\beta$ -alumina samples were acquired at 50-Hz (source) modulation frequency and stored in blank (*B*) and sample (*S*) channels, respectively. Signal ratio (*S/R*) or signal corrected for background ratio [(*S-B*)/*R*] were calculated internally from the stored data.

## Results

Photoacoustic spectra of 2-wt% Cr- $\beta$ -alumina, green and pink forms, are shown in Fig. 1. The peaks reported in the previous study were again observed, but it is clear that both forms show three major peaks in the same regions of the spectrum. A low intensity peak at low energy was observed for the pink form at 570 nm and for the green form at 575 nm. A second peak was

observed at 405 nm for the pink form. The green form exhibited a second peak at 370 nm but a distinct shoulder was seen that could be fit by assigning a peak at 445 nm. A high energy peak below 300 nm was observed for both forms: pink at 225 nm and green at 280 nm.

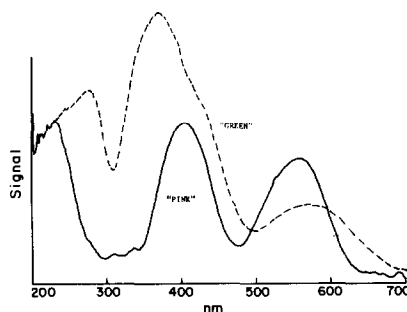


FIG. 1. Photoacoustic spectra for "pink" and "green" chromium-doped  $\beta$ -alumina. Photoacoustic signal is analogous to absorbance.

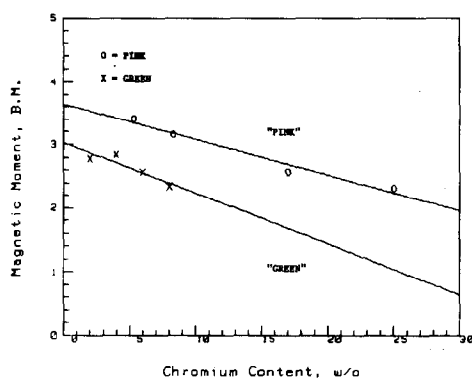


FIG. 2. Magnetic moment for "pink" and "green" chromium-doped  $\beta$ -alumina as a function of chromium content.

The fact that both green and pink forms gave such similar absorption peaks led us to reexamine the other evidence presented earlier. It was true that the air-fired green form could be converted to pink by firing in a stream of 90%  $N_2$ /10%  $H_2$ . However, when the samples were carefully protected from sodium loss by passing the gas stream through a bed of  $\beta$ -alumina before contact with the sample it *never* turned pink (Table I). Without this protection the green form turned pink even when fired in air.

X-ray diffraction patterns were taken of both pink and green forms using a diffrac-

tometer in place of the photographic method used in the earlier study. Both forms showed the presence of  $\beta$ -alumina lines, but the pink form always showed the presence of  $\alpha$ - $Al_2O_3$  lines. In fact, any samples that appeared pink to the eye contained >50%  $\alpha$ - $Al_2O_3$  (Table I). The pinker the samples appeared the higher the percentage of  $\alpha$ -alumina.

Magnetic susceptibility measurements were repeated and the previous results were reconfirmed. Additional evidence was gathered by measuring the magnetic susceptibility as a function of chromium content. This is shown in Fig. 2. At infinite dilution the magnetic moments were closer to spin-only values expected for a  $d^3$  ion (3.87 B.M.) but clearly the green form still exhibited a low magnetic moment.

### Discussion

As in the previous study, the spectroscopic results give the most direct evidence for the oxidation state assignment of chromium. However, now it is clear that both forms exhibit three peaks and both can be fit to an octahedral  $d^3$  configuration using a Tanabe-Sugano diagram as shown in Table II. The only question remaining is the assignment of the middle peak position. As

TABLE II  
SPECTRAL ASSIGNMENTS FOR CHROMIUM-DOPED MATERIALS

	"Pink"		"Green"		
	Observed (nm)	Predicted <sup>a</sup> (nm)	Observed (nm)	Predicted <sup>b</sup> (nm)	Predicted <sup>c</sup> (nm)
${}^4T_{1g}(P)$	225	253	280	268	263
${}^4T_{1g}(F)$	405	403	445 (shoulder) 370 (peak)	445	404
${}^4T_{2g}(F)$	570	573	575	576	581
${}^4A_{2g}(F)$					

<sup>a</sup> Based on fitting of 570- and 405-nm peaks to octahedral  $d^3$  ion.  $Dq = 1757\text{ cm}^{-1}$ ,  $B = 785\text{ cm}^{-1}$ .

<sup>b</sup> Based on fitting of 570-nm peak and 445-nm shoulder to octahedral  $d^3$  ion.  $Dq = 1758\text{ cm}^{-1}$ ,  $B = 453\text{ cm}^{-1}$ .

<sup>c</sup> Based on fitting of 570-nm peak and 408-nm estimated level to octahedral  $d^3$  ion.  $Dq = 1739\text{ cm}^{-1}$ ,  $B = 669\text{ cm}^{-1}$ .

can be seen in Fig. 1 the peak absorption occurred at 370 nm but a shoulder was observed that indicates another peak at 445 nm. The Tanabe–Sugano diagram could not be fit using a peak at 370 nm but fit well with a peak at 445 nm. An alternative assignment can be made by noting that in a distorted octahedral environment the levels will be split (4). If it is assumed that these two peaks are due to splitting the actual  ${}^4T_{1g}(F)$  level should be between the two peaks. If it is assumed to be midway its position would be at  $\sim 408$  nm and a fitting to a  $d^3$  configuration can be made. The resulting assignments are summarized in Table II. The latter assignment agrees well with Cr(III)-doped spinels (5).

It should be noted that green  $\text{Cr}_2\text{O}_3$  also exhibits a peak at 370 nm (6), while Cr(III) doped spinels show a peak near 450 nm (5). X-ray diffraction showed no lines attributable to  $\text{Cr}_2\text{O}_3$  but the possibility of small amounts of  $\text{Cr}_2\text{O}_3$  precipitated at the grain boundaries cannot be ruled out.

As a final piece of spectroscopic evidence it may be noted that the previous study (1) showed little difference between the emission spectra of the pink and green forms.

Based on this overwhelming spectroscopic and X-ray diffraction evidence we now conclude that the green form is Cr(III) in  $\beta$ -alumina while the pink form is Cr(III) in  $\alpha$ -alumina.

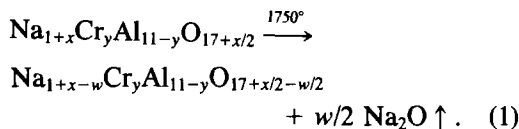
The other evidence supporting, at least indirectly, the previous assignment of Cr(IV) can now be reexamined in light of the spectroscopic results. The value of magnetic susceptibility extrapolated to infinite dilution for the pink form (3.7 B.M.) was nearly equal to the value expected for a  $d^3$  ion (3.87 B.M.) which is consistent with the work of Selwood *et al.* (7). However, the extrapolated value for the magnetic moment of the green form (3.00 B.M.) was still considerably lower than that predicted by the spin-only formula. Again, the early lit-

erature on magnetic susceptibility measurements of chromium oxides provides some consolation. It is well known that the magnetic moment for  $\text{Cr}_2\text{O}_3$  is only 2.76 B.M. (6) but this is hardly magnetically dilute.

A decrease in magnetic moment of  $\text{Cr}^{3+}$  in  $\alpha$ - $\text{Al}_2\text{O}_3$  has been observed with increasing  $\text{Cr}^{3+}$  concentration (7). Decreases in magnetic moments of solid solutions of  $\text{Cr}^{3+}$  in  $\alpha$ - $\text{Al}_2\text{O}_3$  are thought to be due to a nonrandom distribution of  $\text{Cr}^{3+}$  in the  $\alpha$ - $\text{Al}_2\text{O}_3$  lattice (8). This leads to a direct interaction of  $\text{Cr}^{3+}$  ions which tend to collect in pairs along the  $c$  axis (9).

Calculations performed for a random distribution of  $\text{Cr}^{3+}$  in  $\alpha$ - $\text{Al}_2\text{O}_3$  give values very close to those found experimentally, (i.e., 3.74 B.M.), but still slightly lower than spin only values (i.e., 3.87 B.M.) (8). When a nonrandom distribution of  $\text{Cr}^{3+}$  was assumed these calculations yielded magnetic moments of 2.83 B.M. (8) in the same range as the experimental values found here for chromium in  $\beta$ -alumina (Fig. 2).

The slight decrease in conductivity reported previously (2) was observed again in this study. It was also observed that a decrease in sodium content took place when these materials were sintered. It should be noted that sintering Cr-doped  $\beta$ -alumina required somewhat higher temperatures and/or longer sintering times than undoped  $\beta$ -alumina to achieve densities near theoretical. Even when well protected by a bed of  $\beta$ -alumina some of the excess sodium can be lost as shown in Eq. (1):



This loss of sodium would result in a lower concentration of ionic carriers and, hence, to a lower ionic conductivity.

An interesting aspect of this chromium solid state chemistry is the visible color of the materials. It is readily seen from Fig. 1

that there is little difference in the absorption spectra of the pink and green forms, and the assignments given in Table II show that both can be interpreted as octahedral Cr(III) with quite similar  $Dq$  and  $B$  values. Yet, to the eye they appear quite different. This, too, was noted in the early literature, especially with the work of Poole (5), Stillwell (10), and Orgel (11) on chromium doped  $\alpha$ -Al<sub>2</sub>O<sub>3</sub>. The pink ruby form was observed up to a doping level of 8 wt%. Beyond this level the solid solutions were green. It was even found that at high temperatures the pink form will appear to be green (11). A gradual shift in peak position resulted in a remarkable color transition when the peaks reached a certain point.

It was concluded that the substitution of the larger Cr(III) for Al(III) in these materials leads to a "compression" that causes the energy levels to shift gradually with composition or temperature (11). As the compression in the octahedral site increases the more likely is the visible color to be red as observed for Cr<sup>3+</sup> in  $\alpha$ -Al<sub>2</sub>O<sub>3</sub> at low concentrations. For some spinels, on the other hand, the green form is observed at composition >1 wt% Cr (5, 12). Based on these observations and the fact that Cr-doped  $\beta$ -alumina is green at all concentrations studied (as low as 1 wt%) it is likely that the preferred octahedral site is Al (I) near the conduction plane. This site is somewhat distorted and would, therefore, be more likely to give rise to a green color. This conclusion is based on the idea that when the larger Cr<sup>3+</sup> ion (0.65 Å) is substituted for Al<sup>3+</sup> (0.50 Å) in a normal octahedral site the compression effect is large. The resulting color is pink as in Cr-doped  $\alpha$ -Al<sub>2</sub>O<sub>3</sub>. When the site is distorted lattice relaxation may occur resulting in a green color.

The preference of Cr<sup>3+</sup> for the Al (I) site would also help explain the lower than expected magnetic moment. If the Cr<sup>3+</sup> ions tend to pair on opposite sides of the conduction plane their interaction would tend to decrease the observed magnetic moment.

Thus, we conclude that all the evidence gathered to date strongly support the assignment of octahedral Cr(III) in  $\beta$ -alumina doped with chromium.

### Acknowledgments

The authors (J.H.K. and A.M.S.) acknowledge financial support of this project by the National Science Foundation, Grant DMR 80-02676. J.H.K. thanks the University of North Carolina, Chapel Hill, for a visiting professorship which promoted the joint work reported, and the authors thank Dr. R. A. Palmer and Dr. C. H. Lochmüller for the use of the photoacoustic spectroscopy equipment at Duke University.

### References

1. J. H. KENNEDY AND J. R. AKRIDGE, *J. Solid State Chem.* **26**, 147 (1978).
2. J. H. KENNEDY, J. R. AKRIDGE, AND M. KLEITZ, *Electrochim. Acta* **24**, 781 (1979).
3. A. ROSENCWAIG, *Anal. Chem.* **47**, 502 (1975).
4. C. P. POOLE, JR., AND J. F. ITZEL, JR., *J. Chem. Phys.* **39**, 3445 (1963).
5. C. P. POOLE, JR., *J. Phys. Chem. Solids* **25**, 1169 (1964).
6. C. N. RAO AND G. V. SUBBARAO, *Nat. Stand. Ref. Data. Ser. Nat. Bur. Stand. (U.S.)* **49**, 50 (1979).
7. P. W. SELWOOD, L. LYON, AND M. L. ELLIS, *J. Amer. Chem. Soc.* **73**, 2310 (1951).
8. F. S. STONE AND J. C. VICKERMAN, *Trans. Faraday Soc.* **66**, 316 (1970).
9. A. CALLAGHAN, M. J. ROSSITER, AND F. S. STONE, *Trans. Faraday Soc.* **62**, 3463 (1966).
10. C. W. STILLWELL, *J. Phys. Chem.* **30**, 1441 (1926).
11. L. E. ORGEL, *Nature (London)* **179**, 1348 (1957).
12. R. H. ARLETT, *J. Amer. Ceram. Soc.* **45**, 523 (1962).